Applied Catalysis B: Environmental 325 (2023) 122351

Contents lists available at ScienceDirect

Applied Catalysis B: Environmental

journal homepage: www.elsevier.com/locate/apcatb

Molybdenum carbide, supercritical ethanol and base: Keys for unlocking renewable BTEX from lignin

Matthew Y. Lui [a,*], Anthony F. Masters [b], Thomas Maschmeyer [b], Alexander K.L. Yuen [b,*]

[a] Department of Chemistry, Hong Kong Baptist University, Hong Kong
[b] Laboratory of Advanced Catalysis for Sustainability, School of Chemistry, The University of Sydney, Sydney, 2006, Australia

ARTICLE INFO

Keywords:
Lignin valorization
Molybdenum carbide
Ethanol aromatization
Renewable chemicals
Supercritical ethanol

ABSTRACT

Supported molybdenum hemicarbide catalysts were prepared and employed for the depolymerization and deoxygenation of waste lignins to aromatics in supercritical ethanol. Titanium nitride appears be a particularly beneficial support material. Depolymerization at 330 °C led to a higher yield and selectivity for arenes than at 280 °C. Base is essential for efficient substrate conversion: the basic constituents inherent in waste lignins are suitable, as is added sodium hydroxide. Without base, depolymerization is poor, the yield of aromatics is very low, and substrate defunctionalisation does not occur. A significant proportion of aromatic products is formed from supercritical ethanol itself, including benzene, which is likely to be present in all catalytic runs due to ethanol aromatization. Hence the total arene content produced is actually higher than has been widely reported. Catalytic cracking of ethanol leads to C_1-units, which add to reaction intermediates to give aromatics containing odd numbers of carbons (*e.g.* toluene).

1. Introduction

Climate change, coupled with dwindling conventional fossil oil resources, is one of the greatest existential challenges facing humanity in the 21st century. The rapid development of methods for the production of carbon-based chemicals and fuels from non-fossil sources, such as waste biomass and carbon dioxide, represents one of the most direct pathways for reducing the carbon footprint of the Chemical Industry, without losing the advantages that this industry affords us.

To date, much of the successful progress reported has been focused on the preparation of platform chemicals from biomass-derived carbohydrates. These bio-derived chemicals include bio-ethanol, 2,5-furandicarboxylic acid (2,5-FDCA), levulinic acid, and succinic acid: all of which are being, or are planned to be, produced at large industrial scales. Amongst the aforementioned examples, 2,5-FDCA is an excellent candidate as a potentially disruptive "drop-in" replacement for 1,4-benzenedicaboxylic acid for the production of polyethylene terephthalate (PET) [1]. Many technical barriers, however, will need to be surmounted before such substitutions are widely adopted. An alternative with potentially lower barriers to market entry would be to develop efficient methods for the conversion of waste biomass to those chemicals, which are already being used for large-scale applications: so called "like-for-like" replacements of petrochemicals.

In addition to studies on carbohydrate and lipid processing, the conversion and upgrading of lignin, which comprises up to 30 wt % of woody biomass, has become an intensive area of research, as lignin is the largest pool of regenerable aromatic compounds in nature. An estimated 50 million tonnes of Kraft lignin is produced annually as a by-product of the pulp & paper industry [2]. Despite its availability, lignin is currently the least valorized fraction of lignocellulosic biomass. Approximately 95 % of all Kraft lignin is burnt as boiler fuel for energy recovery; and used as a reductant for the regeneration of pulping chemicals [3], rather than being upgraded to chemicals of higher value [4]. The selective depolymerization of lignin, while preserving its aromatic nature, is highly desirable. However, due to its structural complexity and non-regularity, as well as its propensity for repolymerization [5], lignin conversion to platform chemicals with high selectivity has proven to be much more difficult than is the case when using carbohydrate-based biopolymers.

The solvolysis of lignin is one of the most common ways to depolymerize lignin. In contrast to the pyrolysis method, solvolysis in hydrogen-donating solvents produces low quantities of char. This important observation was reported by Bai and co-workers, who used isopropanol and tetralin for the liquefaction of Organosolv lignin into short chain vinyl- and alkyl-phenols under flow conditions at

* Corresponding authors.
E-mail addresses: matthew-lui@hkbu.edu.hk (M.Y. Lui), alexander.yuen@sydney.edu.au (A.K.L. Yuen).

https://doi.org/10.1016/j.apcatb.2022.122351
Received 24 October 2022; Received in revised form 16 December 2022; Accepted 29 December 2022
Available online 9 January 2023

300–400 °C. In their study, the yield of aromatics (mostly substituted phenolics) was reported to be approximately 10 wt % of the lignin feedstock [6]. Hydrothermal liquefaction of lignin and lignocellulosic feedstocks is another method which has been explored by several groups in depth [7]. A common observation from these studies is that the addition of a base is important for suppressing char formation. Catalytic hydrothermal conditions strongly favour the conversion of lignin to phenolic products, such as vanillin, guaiacol and catechol derivatives, rather than arenes. Mixed water–ethanol systems at 310 °C also tend to afford phenols and oxygenated aromatics [8].

From an industrial perspective, selective conversion to arenes rather than phenolics is favoured, due to the volume of non-oxygenated arenes required for a large number of end applications. Benzene and alkyl benzenes, especially BTEX (benzene, toluene, ethylbenzene and xylenes) are very significant, high-volume products obtained from the refining and subsequent upgrading of crude oil. The worldwide annual demand for BTEX in 2014 was approximately 115 million tonnes [9]. Benzene and alkyl benzenes are components in liquid fuels (*i.e.* gasoline, diesel and jet fuels) [10], and starting materials for a large number of important industrial chemicals (Fig. 1). The major production pathway for BTEX currently is the catalytic reforming of naphtha as part of standard petroleum refinery operations.

Hence, the discovery of an efficient method which selectively generates replacements for petroleum-derived platform-chemicals from waste biomass, using water or renewable alcohol(s), would facilitate the development of a commercial-scale biorefinery. Recent literature revealing the possibility of producing BTEX from lignin, includes the work by Meng et al., who demonstrated that Organosolv lignins can be converted into benzene (18.8 wt %) under hydrothermal conditions (180 °C) in the presence of an HY zeolite supported RuW alloy catalyst. Their combined experimental/DFT mechanistic study indicated that the Brønsted-acidic zeolite catalyzed the scission of C_{sp2}–C_{sp3} bonds, while the RuW acted as an efficient self-supported hydrogenolysis catalyst for the cleavage of C_{sp2}–O bonds [10].

Catalytic ethanolysis of lignin has been studied by a number of research groups. Hensen and co-workers subsequently reported the methanolysis and ethanolysis of soda lignin under supercritical conditions with a $CuMgAlO_x$ catalyst [18]. Ethanol was a more effective solvolysis agent than methanol, affording up to 23 wt % yield of monomeric products at 300 °C, compared to 6 wt % yield under comparable methanolysis conditions. Running their process at temperatures of 340–420 °C, resulted in improved yields of monomeric products. For soda lignin, optimal monomer yields of 60 wt % were reported at 380 °C after 8 h in ethanol [19]. Alkylbenzenes constituted slightly less than 25 % of these monomers at 340 °C, increasing to 38 % at 380 °C. Overall, the product suite contained at least 26 distinct species, including, phenols, benzyl alcohols, methylphenyl ethers, as well as hydrogenated (aliphatic) 6-membered rings. Further studies by Hensen and co-workers have demonstrated that the distribution of these monomeric products is adjustable and that their catalytic system was suitable for Kraft lignin depolymerization, resulting in an impressive conversion to 86 wt % monomers, of which 35 wt % were alkylbenzenes [20].

Recently, Li and co-workers reported the use of a series of supported molybdenum catalysts for Kraft lignin ethanolysis under supercritical conditions [21,22]. High conversions of lignin to aromatic monomers (within a more complex product suite) were achieved. At 280 °C, α-MoC_{1-x}/AC and Mo/Al_2O_3 gave 28.0 wt % [21] and 33.2 wt % [22] aromatic yields respectively. These monomeric products include alkyl benzenes, benzyl alcohol derivatives and guaiacol derivatives. To improve the conversion, Li and co-workers investigated the ethanolysis with an α-MoC_{1-x}/Cu-$MgAlO_z$ composite catalyst [23], which combines the virtues of each reported individual catalyst type [18,21]. Using this composite catalyst and higher temperature (330 °C), a high yield of aromatic monomers was achieved (575 mg/g lignin), although the direct conversion of ethanol to benzene under these conditions was not taken into account in estimating the yield. Two classes of aromatic products were produced: namely alkyl benzenes and benzyl alcohol derivatives. When using enzymatically hydrolysed lignin, Li et al. reported that in the ethanolysis involving tungsten-[24] and nickel-based [25,26] catalysts, the majority of the products were phenolic compounds, in contrast to the BTEX products of their former studies involving the conversion of Kraft lignin with molybdenum carbide.

Our group previously reported the use of delaminated molybdenum sulfide (MoS_2) and bulk or supported molybdenum hemicarbide (Mo_2C) as catalysts for the ethanolysis of Kraft lignin [27]. Molybdenum hemicarbide was found to be a particularly efficient heterogeneous catalyst for reductive depolymerization of Kraft lignin, being tolerant of the various sulfur-containing functional groups present which contributed to a total sulfur content of 2.80 wt % in the commercially available material. Additionally, the Mo_2C-based catalysts were tolerant of the high inorganic content of Kraft lignin (19.4 wt % ash). Despite attractive aromatic monomer yields of 419–425 mg/g lignin under Mo_2C catalysis at 280 °C in ethanol, the system suffered from two principal disadvantages. The first was the limited extent of lignin liquefaction (64 % of insoluble lignin converted to small molecules and soluble oligomers); the second was incomplete deoxygenation of aromatic monomers in the product suite. For example, unsupported Mo_2C at 280 °C resulted in a 53:47 ratio of arenes to monooxygenates (benzyl alcohols and 2-methylbenzaldehyde). The current study, addresses these two limitations and extends the scope of our catalysis to Protobind (Soda-pulp) and Organosolv lignin, black liquor derived from mixed Eucalyptus wood, as well as sodium lignosulfonate: a useful by-product of the sulfite pulping process [28]. The effects of substrate acidity and basicity on lignin conversion are explored, as well as some fundamental experimentation using monomeric and dimeric lignin model compounds, and reactions of solvent ethanol itself, to gain mechanistic insights into the catalytic steps.

The effect of the catalyst–support interaction was also investigated using three distinct systems: metal oxide (alumina), metal nitride (TiN) and an unsupported Mo_2C.

2. Experimental section

The details of the experimental procedures below are taken in part from the Thesis of one of our recent PhD graduates,[1] which includes related catalytic studies of molybdenum sulfide catalysts, and in part from our previously published work [27].

2.1. Materials

Kraft lignin (Catalogue # 471003), sodium lignosulfonate (Catalogue # 471038); ethylbenzene, propylbenzene, 2-methyl benzyl alcohol 2-methylbenzaldehyde, guaiacol, 2-methyl benzyl alcohol, 1-ethyl-3-methyl benzene, 4-methylguaiacol, 4-ethylguaiacol, 4-propylguaiacol, 3,4-dimethoxybenzyl alcohol; ammonium heptamolybdate and melamine were purchased from Sigma–Aldrich. Ethanol, toluene, benzene, benzyl alcohol and naphthalene were obtained from Merck. *p*-Xylene and *o*-Xylene were purchased from Fluka and Alfa Aesar, respectively. 2,4-Dimethyl styrene was obtained from Enamine Ltd 3-Methyl propylbenzene was purchased from Combi-Blocks Inc. 1-Ethyl-2,4-dimethyl benzene was purchased from Fluorochem Ltd. Samples of Protobind and Organosolv lignin were purchased from Green Value Pty Ltd. Eucalyptus black liquor was supplied by the CSIRO, Australia. Cubic TiN (powder, 20 nm) was purchased from US Research Nanomaterials Inc. (Product# US2060). Basic alumina (Catalox® SBa-150) was obtained free of charge from Sasol Ltd. Unless otherwise stated, all chemicals were used as received. The β-O-4 linkage model, 1-(3,4-dimethoxyphenyl)−2-(2-methoxyphenoxy)propane-1,3-diol (**16**), was

[1] J. Strachan. On Molybdenum Sulfides and Other Active Materials for Sustainable Energy Systems. PhD, The University of Sydney, Sydney, 2020.

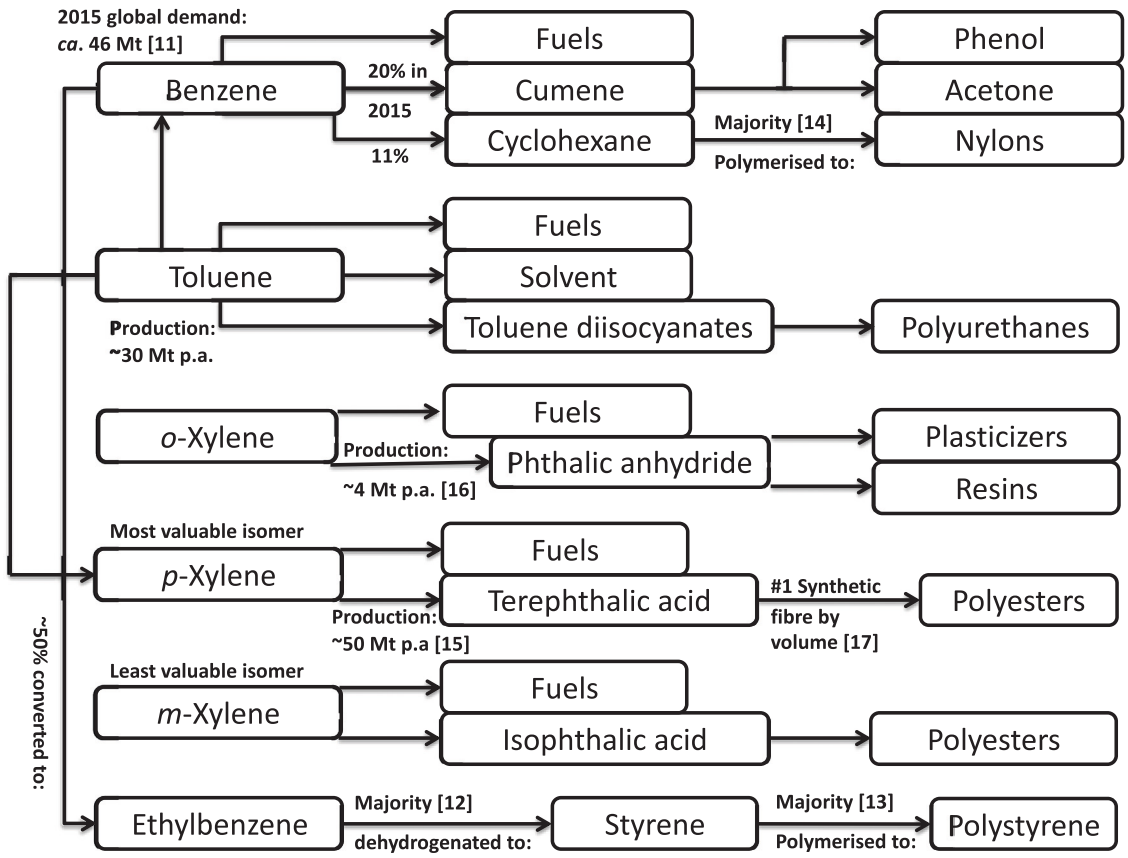

Fig. 1. Major platform chemicals in the BTEX chain. Selected production and conversion values given [11–17].

prepared as a racemic mixture according to literature procedures [29] (See Supporting Information).

2.2. Catalyst preparation

Mo_2C and $Mo_2C@Al_2O_3$ were prepared using methods described previously [27]. $Mo_2C_{1-x}N_x@TiN$ was prepared similarly, using a modified version of the methods originally reported by Pang and co-workers [30]. In order to determine the molybdenum loading, several batches of unsupported Mo_2C were prepared by thermal decomposition of the melamine–molybdate coordination polymer as described below. The averaged mass ratio of this precursor to the product Mo_2C was then used to determine the required mass-ratio of the support material to the melamine–molybdate coordination polymer in the synthesis mixture, such that the final Mo-loading in the supported catalysts was 30 wt %. Accordingly, the melamine–molybdate coordination polymer was co-ground with nanoparticulate TiN and the mixture thermally decomposed under flowing H_2 in Ar (*ca.* 2:5 ratio; 70 mL min^{-1}), with a heating ramp rate of 5 °C/min and subsequently held at 650 °C for 1 h. The sample was cooled to room temperature under Ar, then the gas flow ceased, and back-diffusion of air allowed for several hours before collection of the sample from the furnace at ambient temperature. The alumina-supported catalyst was prepared similarly.

2.3. Catalyst characterization

Catalyst surface areas were calculated by analysis of N_2 sorption isotherms using a Micrometrics Accelerated Surface Area & Porosimetry System (ASAP) 2020 instrument, using the Brunauer–Emmett–Teller (BET) model in the accompanying Micrometrics software package. The powdered sample was initially outgassed (90 °C and 13 μbar), then dried at 200 °C for several h until the measured outgassing rate over a 30 s period was negligible. N_2 adsorption and desorption was performed at 77 K.

Powder X-ray diffraction (PXRD) was performed on catalyst loaded into 0.5 mm quartz capillaries, using a Stoe Stadi P diffractometer equipped with a Mo X-ray source, operating in transmission mode (Debye–Scherrer geometry). The data were analyzed by HighScore Plus version 3.0e software and plotted using Origin 9.6.5.

Transmission electron microscopy (TEM) was conducted on a JEOL-TEM-2100 operated at 200 kV. Samples were prepared by dispersing a few mg of powdered catalyst in absolute ethanol, briefly sonicated and 10–20 μL of suspension was immediately drop-cast onto 300 mesh copper grids pre-coated with formvar films and holey carbon. Electron energy loss spectroscopy (EELS) was conducted on a JEM-2200FS (200 kV) spectrometer equipped with an in-column omega filter, at an energy resolution of 1 eV, using condenser lens #3, with a convergence angle of approximately 38 mrad and a collection angle of approximately 170 mrad.

2.4. X-ray absorption spectroscopy

Molybdenum K-edge XAS data were collected in transmission mode at the XAS beamline at the Australian Synchrotron. The photon delivery system comprised a 1.9 T wiggler and step scanned Si(311) monochromator. A sample of molybdenum foil was simultaneously measured as a reference to account for beamline energy drift. Samples were packed into open-ended quartz capillaries with glass wool which allowed the flow of gases through the sample during analysis. To observe the reducing effect of ethanol at high temperature on the catalyst, N_2 was bubbled through ethanol and hence the atmosphere passing over the samples contained ethanol vapour. The portion of the sample in the beam path was heated to 300 °C with a hot air blower (measured using a thermocouple). The XAS data were analyzed using the IFEFFIT packages

of Athena and Artemis.

2.5. Lignin drying and ashing

In the cases where dried lignin was used as a substrate, samples of Kraft, Organosolv and Protobind lignins were dried in an oven at 140 °C for 24 h. Aqueous Eucalypt Black Liquor was acidified to pH 1 with concentrated hydrochloric acid and the resulting precipitate filtered off, washed with water and dried as described above. Inorganic ash content was determined by calcining non-dried samples in a tube furnace, under ambient atmosphere at 800 °C for 4 h or for precipitated Black Liquor, by means of thermogravimetric analysis. Ash and moisture contents were determined to be:

	Kraft	Organosolv	Protobind	Black Liquor
Moisture (wt %)	16.0	5.57	9.19	4.5
Ash (wt %)	19.4	< 0.1	18.2	0.74

2.6. Catalysis

All ethanolysis processes were conducted in a Hastelloy C Parr reactor system. This system incorporated a thermowell, mechanical stirrer and cooling loop. Lignin samples (1.0 g), catalyst (160 mg for unsupported Mo_2C; 500 mg for supported catalysts), and absolute EtOH (100 mL) were added to the reactor vessel. It was then sealed, pressurized with N_2 to 50 barg, followed by release (3 cycles) and finally *ca* 1.4 barg of N_2 was introduced. The reaction mixture was stirred at 700 rpm and heated to supercritical conditions over a period of *ca*. 1.5 h, held at the desired temperature and autogenous pressure for up to 6 h, then the heating jacket removed to initiate the cooling step. A water bath was used to shorten the cooling time once the internal reactor temperature was below 200 °C. Upon cooling, the reactor was depressurized and unsealed. The product mixture was then filtered under reduced pressure. The residual material was washed with excess EtOH and dried at 80 °C overnight. External standard dibenzyl ether (20 μL) was introduced, and the final volume of the product mixture was adjusted to 200 mL in a volumetric flask with EtOH. In preparation for the subsequent catalytic run, the reactor head-space was cleaned using supercritical MeOH (100 mL; 250 °C; autogenous pressure >82 barg; 30 min; 2 times). Mechanistic studies using substrates other than lignin and controls runs performed in the absence of substrate were conducted under otherwise identical conditions to those described above.

For reactions in which sodium hydroxide was added in place of basic lignin, the amounts of NaOH were calculated to be approximately the same as would be present in 1.0 g of dried Kraft lignin (see above), being approximately 250 mg for 100 mL of ethanol. In the case of reactions scaled down to 550 mg of substrate, both the base as solvent were scaled accordingly 140 mg of NaOH and 55 mL of ethanol.

2.7. Reaction analysis

As per our previous study [27], product quantitation was carried out on a Shimadzu GCMS-QP2010 equipped with Rtx-5MS 0.25 μm × 30 m × 0.25 mm column. The sample was volatilized at 250 °C or at 300 °C, held in an isothermal step at 50 °C for 3 min, heated to 330 °C at a rate of 10 °C.min^{-1}, and held at 330 °C for 10 min. The chemical substances in the product mixtures were identified by comparing the retention time and EI-MS spectra of authentic samples and with those in the NIST05 database. Of the 12 common, prominent aromatic species identified, quantification using calibration curves of authentic samples (see text) was performed. On the basis of structural similarity/isomerism, product **7** was assumed to have the same molecular response as **6**, and similarly, products **9**–**11** to have the same molecular response as product **8**. Dibenzyl ether was employed as the external standard.

3. Results and discussion

3.1. Catalysts & reaction system

Our previous lignin valorization study [27] established that molybdenum hemicarbide-based catalysts and supercritical ethanol were effective for the depolymerization and removal of heteroatoms from commercial Kraft lignin. This system addressed several of the challenges required for lignin processing: an earth-abundant, sulfur tolerant catalyst; preferential chemoselectivity for hydrogenolysis over hydrogenation; use of renewable ethanol as transfer hydrogenolysis agent, and good yields of monoaromatic products. Nevertheless, several key questions remained, not the least of which concerned reaction mechanisms and optimization of conditions. The sequence and order of steps leading to the successful deoxygenation and desulfurization of the oligomeric lignin fragments resulting from thermolysis were unclear. The several roles the solvent, supercritical ethanol, played in the process also needed to be understood. In addition, whether and, if so, which, catalyst supports could be used to further enhance Mo_2C-based materials for arene production were underexplored.

With these goals in mind, we set out to prepare catalysts with beneficial synergies between the support and the molybdenum phase and test them using our established lignin depolymerization conditions. Compared to the parent Mo_2C, two other candidates were chosen based on an initial catalytic performance: Mo_2C supported on basic alumina (Mo_2C@*b*-Al_2O_3) and what was initially thought to be Mo_2C supported on titanium nitride, but is better described as a molybdenum carbonitride–TiN composite (see below). Both materials were prepared from the thermal decomposition of a melamine–heptamolybdate coordination polymer [30] on the support material at 650 °C.

Powder X-ray diffraction analysis revealed the presence of the expected molybdenum hemicarbide phases in all three samples (Fig. 2). Although the γ-alumina used as a support was not crystalline, evidence of its effect on the carbide phase was apparent in the small amount of molybdenum oxide formation that was evident in terms of a reflection at *ca*. 12° 2-theta. For the TiN supported material, the nanoparticulate nature of the support led to significant broadening of the expected reflections from the support phase, however, Rietveld refinement of the data indicated clearly that both phases were present.

The BET surface areas of all the catalysts were measured by N_2 sorption and found to be less than 10 m^2/g and below 40 m^2/g for the unsupported and TiN-supported materials, respectively (Table S1). These rather low values were consistent with what had been reported previously, as the decomposition of the melamine–heptamolybdate precursor is reported to give material that is compact, non-porous and free from excess surface carbon [27,30]. In the case of the alumina-supported material, the measured value of 107 m^2/g revealed that despite the density of the catalyst and its tendency to clump on the

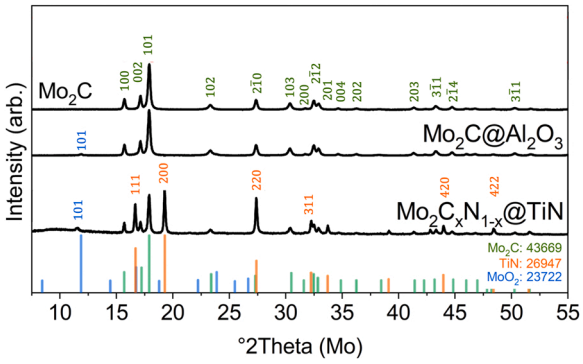

Fig. 2. Indexed PXRD diffractograms of catalysts Mo_2C, $Mo_2C@Al_2O_3$ and $Mo_2C_{1-x}N_x$@TiN at 25 °C, with their reference peaks from ICSD entries indicated at the bottom right.

support (see Fig. 3, **(b)**), the particles were small enough that they did not completely diminish the inherent surface area of the alumina used (S_{BET} 150 m^2/g). These surface area measurements were supported by TEM analysis, which revealed the morphologies of the 3 materials, as shown in Fig. 3.

As observed previously [27], the unsupported Mo_2C appears to be bulky and dense. This morphology remains when alumina was used as the support. Although the contact between the two phases appears limited, evidence of interaction was observed by examining the powder X-ray diffraction data (shown in Fig. 2). Some evidence of oxidation of the molybdenum is evident in the alumina supported material, however, this did not significantly reduce the efficacy of this catalyst (see below). The catalyst surface is expected to be stripped of oxide under the reductive reaction conditions, hence the main influence of the alumina support appears to be as a dispersant for the Mo_2C particles. In contrast to the other two catalysts, titanium nitride-supported material consisted of smaller nanoparticles overall. In this sample the difference between the molybdenum carbide and titanium nitride phases was less obvious. EELS analysis of this sample revealed co-localization of the molybdenum and titanium in this material. Further sample analysis of the TEM images revealed that the presence of titanium nitride led to the formation of a of a core–shell structure in which the molybdenum carbide-rich phase is finely dispersed on the surface of the TiN, henceforth denoted as $Mo_2C_{1-x}N_x$@TiN in which a substantial amount of nitrogen was incorporated into the molybdenum phase. Based on this evidence we hypothesize that the number of accessible active sites in the $Mo_2C_{1-x}N_x$@TiN catalyst is greater than in the other two catalysts. Nitrogen doping of the molybdenum carbide is also anticipated to increase its efficiency for hydro-deoxygenation and -desulfurization due to tuning of the electronics at molybdenum [31].

In addition to the catalytic studies reported here, this molybdenum carbo-nitride was characterized by XAS at the Australian Synchrotron, and by variable temperature XRD, XPS & TEM as part of ongoing studies within our laboratory. Full descriptions and analyses of our structural investigations will be published separately.

The X-ray Absorption Near Edge Structure (XANES) regions of the as-synthesized catalysts (supported on Al_2O_3 and TiN) at 25 °C and 300 °C under a stream of ethanol in nitrogen, compared to Mo-foil, were measured and are reported in detail elsewhere. As shown in Fig. 4, the absorption edge for the unsupported Mo_2C sample was the lowest of the three samples examined, at 20.012 keV, consistent with an oxidation state of *ca.* Mo(1.25). At 300 °C, very little change in edge energy was observed. In contrast, both the supported samples had higher energy edge positions at 20.014 keV for Mo_2C@*b*-Al_2O_3 and 20.016 keV for $Mo_2C_{1-x}N_x$@TiN. The higher energy edge shifts for the supported materials indicated that the apparent oxidation state of Mo was approximately Mo(3.5) in both Mo_2C@*b*-Al_2O_3 and $Mo_2C_{1-x}N_x$@TiN, and hence there was less electron density at Mo in these samples compared to unsupported Mo_2C. When heated under ethanol, the electron density increased, with the alumina-supported catalyst changing apparent oxidation state to *ca.* Mo(2) and that of the titanium nitride-supported material to Mo(3).

Having prepared and characterized the catalysts, lignin reductive ethanolysis studies were commenced using the protocol established

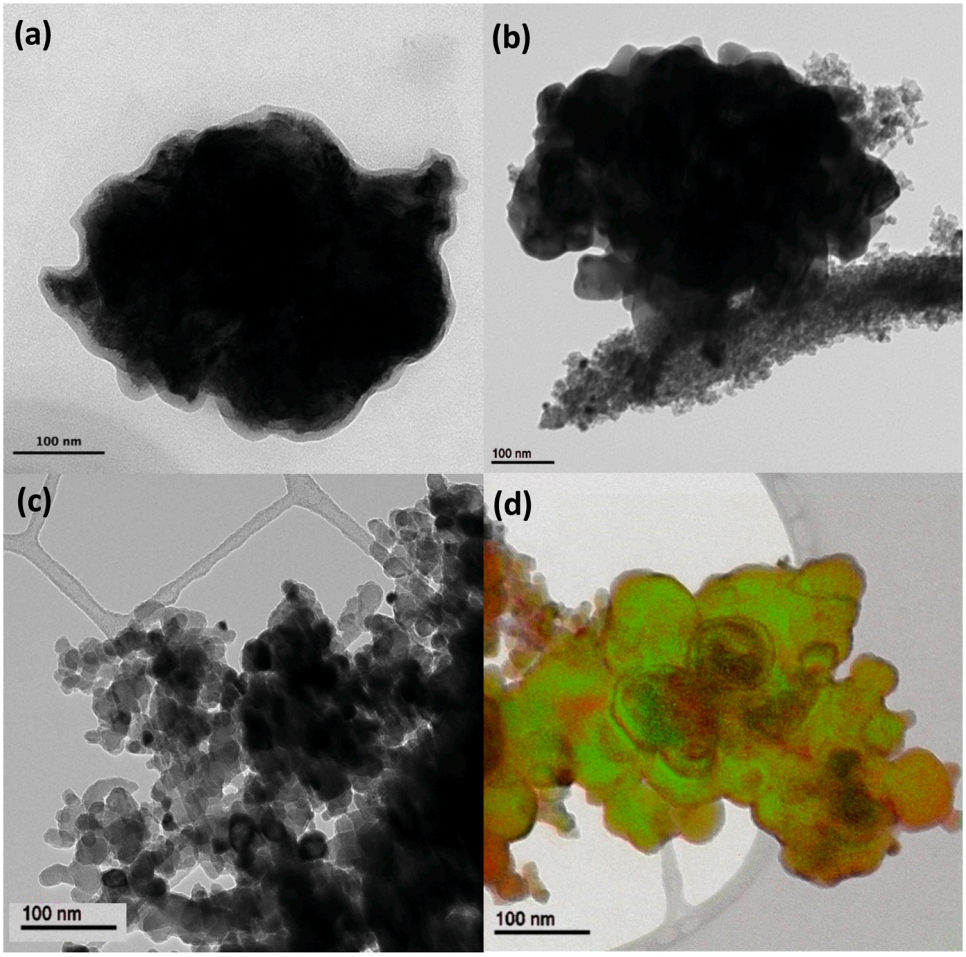

Fig. 3. Bright field TEM micrographs of the catalysts prepared for lignin conversion. Unsupported Mo_2C **(a)**; basic-alumina supported Mo_2C **(b)**; TiN supported molybdenum carbo-nitride **(c)** and Electron Energy Loss Spectroscopy (EELS) for this sample **(d)**: *red* = Ti, *green* = Mo.

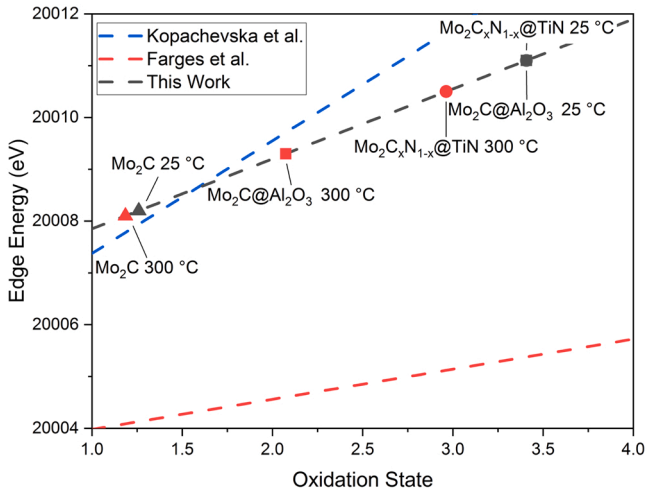

Fig. 4. Mo oxidation state *vs.* K-edge energy comparison of the literature with this work. Kopachevska et al. [32], Farges et al. [33].

previously [27]. The process is depicted in brief in Fig. 5.

The reactor was charged with solvent, catalyst and starting material, the oxygen in the head-space and dissolved in the solvent was removed, then the reaction commenced under a low pressure nitrogen atmosphere. Upon heating to the desired set temperature, the autogenous pressure reached was in the range of 150–200 bar: well above the critical pressure of ethanol (61.4 bar) [34]. Although it has been reported that the solubility of lignin is high under supercritical conditions [35], we were not able to find any published quantitative solubility data, recognizing that lignin solubilization inevitably also involves some reaction with the supercritical medium.

Post-reaction, the gas fraction was not recovered for analysis. However in one instance, bubbling the entire reactor head pressure through an aqueous solution of copper(II) sulfate did not reveal the presence of hydrogen sulfide or other reactive, volatile sulfur species in the gas phase. This substantial lack of sulfur in the gas phase is in line with the observations of Li and co-workers [36] and others [37].

We also employed a reaction temperature of 330 °C to compare the performance at two temperatures for unsupported and basic alumina-supported Mo_2C (Table 1 below), enabling comparison with recent work by Li et al. [23].

As it was apparent from the negative control runs that this simple increase in temperature improved selectivity for monoarenes (BTEX-type) compared to oxygenates (benzyl alcohols and benzaldehydes), the $Mo_2C_{1-x}N_x$@TiN catalyst was evaluated only at 330 °C. The effects of reaction temperature on substrate deoxygenation are further discussed below in the context of our investigations into the reaction cascade using lignin model compounds.

Table 1
Overview of Kraft lignin processing to single-ring aromatics in supercritical ethanol with catalysts.[1]

Catalyst	Liquefaction (%)[2]	Oxygenates (mg/g)[3]	Arenes (mg/g)[3]	Total (mg/g)
None added	**85**	**77**	**25**	**102**
(**negative** Control)				
280 °C				
330 °C	**80**	**21**	**253**	**274**
TiN	**80**	**142**	**224**	**366**
(**positive** Control)				
330 °C; dry KL[4]				
Mo_2C	**64**	**201**	**226**	**427**
280 °C				
330 °C	**82**	**42**	**499**	**541**
Mo_2C@*b*-Al_2O_3	**68**	**250**	**166**	**416**
280 °C				
330 °C	**100**	**24**	**579**	**603**
$Mo_2C_{1-x}N_x$@TiN	**100**	**0**	**666**	**666**
330 °C				
$Mo_2C_{1-x}N_x$@TiN	**100**	**0**	**709**	**709**
330 °C; dry KL[4]				

[1] Kraft lignin (1.0 g), EtOH (100 mL), catalyst (15 wt % loading of Mo with respect to lignin) were heated to 330 °C under initial pressure of *ca*0.1.4 bar and final pressure of 110–190 bar N_2 for 6 h.
[2] Liquefaction extent is used as an indication for substrate conversion (see text).
[3] Both aromatic and non-aromatic products (arising from EtOH are present). Aromatics were identified and quantified as described in the Experimental Section and are expressed as mg of product per g of lignin.
[4] Lignin dried at 140 °C for 24 h.

3.2. Catalytic processing of kraft lignin

In Table 1, 'liquefaction': the extent to which the organic substrate is solubilized, is presented as a measure of the extent to which the reaction has progressed. Because uncatalyzed reactions of the substrate occur under supercritical conditions, it is not meaningful to use the conventional parameter 'conversion' as measure of the progress of the catalysed reaction.

For example, both depolymerization and repolymerization of the starting lignin under supercritical conditions may proceed concurrently, "converting" the starting lignin to a different lignin-type substrate. We envisage that after the initial fragmentation of the substrate in supercritical ethanol, the failure to remove reactive functional groups by either solvolysis or catalytic reduction results in oligomer

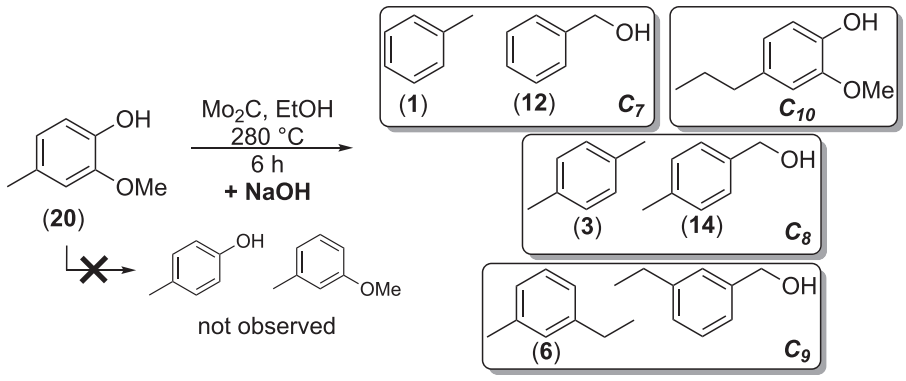

Fig. 5. Catalytic conversion of waste lignin in supercritical ethanol.

repolymerization by means of radical coupling. This repolymerized material has a more condensed structure than the lignin substrate and is hence more intractable, recalcitrant and acts as a potential inhibitor of further catalysis. Accordingly, the observation of limited substrate liquefaction was interpreted as a reliable indication that the desired solvolysis and heteroatom removal had not been extensive.

Despite increasing the yields of monoaromatic products, the presence of the catalyst and support are not necessarily beneficial for substrate liquefaction. At 280 °C, both unsupported Mo_2C and Mo_2C@*b*-Al_2O_3 appeared to inhibit liquefaction compared with the negative control conditions. We could not determine whether the diminution in liquefaction was due to prevention of polymer fragmentation or the promotion of repolymerization of soluble lignin fragments. Whichever the case, the effect was no longer observed at 330 °C, with liquefaction being equal or greater than the negative control conditions at the equivalent temperature. From these data in isolation, however, it was difficult to reconcile the apparent high yields of aromatic products given the mass of remaining lignin. Further experiments with just ethanol and an unreactive substrate were performed to determine the origins of the high arene yields. The results of these, along with in-depth discussion of this observation are set out below in the section devoted to the elucidation of the several roles ethanol plays in the reaction.

A significantly greater yield of aromatics was observed in the presence of the titanium nitride support (positive control) compared with an absence of catalyst (negative control), without markedly affecting liquefaction. This indicated that TiN itself likely played a beneficial role in the process: increasing yield and selectivity to arenes. Nevertheless, additional synergies were clearly observed in the presence of molybdenum carbo-nitride, as the yield and selectivity to arenes increased further when $Mo_2C_{1-x}N_x$@TiN was employed compared to the TiN support alone. Unsurprisingly, the use of the same mass of pre-dried lignin marginally improved the yield of arenes due to the increased input of organic starting material.

The chemical species that made up the monoarene and oxygenate fractions in Table 1 were identified by GCMS and are given below, with their respective compound numbers which are used throughout the discussion, in Fig. 6 along with the total relative proportions of each fraction for each set of conditions. For quantification of the aromatic species, authentic standards of the 7 arenes and 3 oxygenates shown in Fig. 6 (*top*) were used. 3-ethyltoluene (**6**) was also used as a calibrant for its C_9-isomer (**7**) and similarly, compound **8** was used as the calibrant for all C_{10}-isomers identified. These arenes and oxygenates proved to be the common products across all the catalytic runs performed in this study (See also Table S2 **& S3**).

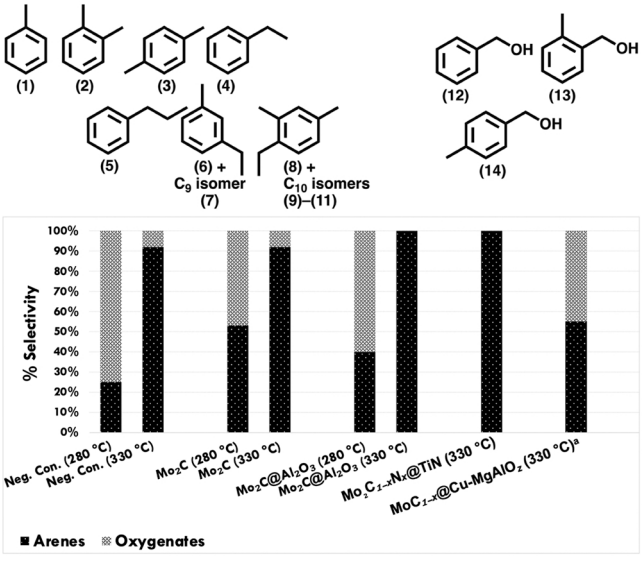

Fig. 6. *Top*: Identity of arenes (**1**–**11**) & oxygenates (**12**–**14**) within the aromatic product stream (compound numbers here used throughout the discussion); *Bottom*: proportions of these fractions and, [a]data reported by Li and co-workers. [23].

The trend for increased deoxygenation with increased reaction temperature is clear from Fig. 6 (*bottom*). Moreover, the use of the supports enhances this deoxygenation to the point that the selectivity is very high for single ring arenes using basic alumina and titanium nitride as support materials. With the $Mo_2C_{1-x}N_x$@TiN catalyst, the selectivity for arenes over oxygenates surpassed the system of Kim et al., who reported *ca.* 450 mg of aromatics per gram of lignin with a 59:41 arene: oxygenate ratio [38], and also surpassed one of the best systems reported to date: that of Li and co-workers, who made use of a carbon-deficient MoC phase supported on a copper-doped hydrotalcite [23]. Looking more closely at the details of the arene products resulting from $Mo_2C_{1-x}N_x$@TiN catalysis, approximately 70 % of the observed alkyl benzenes belonged to the BTEX group. In fact, across all the examples in this study, a large proportion of the arenes isolated contain multiple alkyl side-chains of 1–3 carbons. Several possibilities for their presence are hypothesized. They could have (A) come from lignin itself: the result of defunctionalization of the non-aromatic functionality originally present; (B) been the result of ethanol deoxygenation and cracking, followed by addition of intermediates to lignin-derived arenes already present in solution; or (c) been derived solely from ethanol. Several tests were performed to distinguish which possibility was the most likely (see below) as part of our mechanistic investigations.

3.3. Reductive depolymerisation of other lignins

The scope of the $Mo_2C_{1-x}N_x$@TiN catalyst was probed, under standard reaction conditions, to determine whether certain lignin types were more suitable than others as a source of arenes. Although Kraft lignin is the largest source of industrial lignin, its structure is significantly modified by the pulping process compared to that of native lignin[3] and it also contains a large proportion of inorganic material. Calcination at 800 °C of the Kraft lignin used in this study resulted in 19.4 wt % of the sample remaining as non-volatile, inorganic residue. Similarly, lignosulfonates recovered from sulfite pulping processes also contain a significant amount of inorganic material. The results of processing several different types of lignin are shown in Fig. 7. It is worth noting that despite the variation in aromatic yields and extent of liquefaction, the process was at least 96 % selective for arenes for all lignin sources. In general, minimal amounts of oxygenates were observed. Dried Kraft lignin yielded 709 mg of arenes per gram of lignin under the same conditions as outlined in Table 1. Sodium lignosulfonate and Eucalyptus lignin recovered from black liquor (BL) also gave high yields of arenes, indicating that our catalytic system was robust and could handle outputs

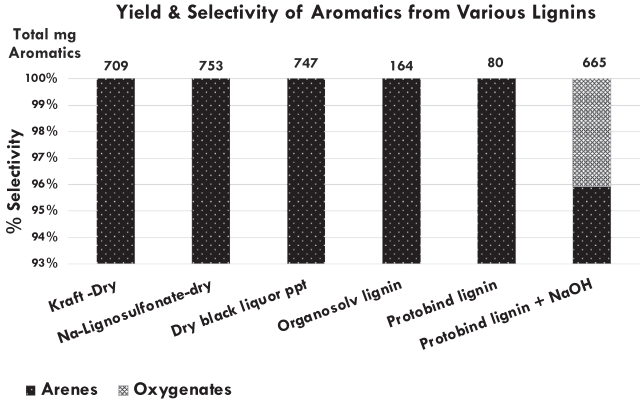

Fig. 7. Yields and selectivity of arenes derived from various lignin sources using $Mo_2C_{1-x}N_x$@TiN in supercritical ethanol at 330 °C.

from various types of pulping waste streams. Surprisingly however, Organosolv and Protobind lignins, which retain the majority of their 'native' structure and are non-sulfurous, were resistant to our process conditions. Despite retaining most of their relatively reactive β-O-4 linkages, Organosolv and Protobind lignins did not completely liquefy (82 % and 78 % respectively) and afforded only very low yields of arenes (164 mg & 80 mg, respectively). Of these two substrates, Despite Protobind being insoluble in water at room temperature, it was found to contain 18 wt % inorganic material: more than aqueous-soluble for Kraft lignin. Hence the ash content of Protobind did not appear to be inherently basic and the organic fraction is known to contain acidic functional groups. Given the fact that all previous successful depolymerizations had occurred with samples containing a significant amount of basic, inorganic residue and that the origin of this residue was from the basic conditions used in the pulping process, it seemed likely that the presence of base was a necessary requirement for successful decomposition of the substrate. Accordingly, sodium hydroxide was added to the reaction mixture (250 mg, being *ca.* 20–25 wt % of the substrate: in line with the amount of inorganic residue present in dried Kraft lignin). This resulted in a marked improvement for Protobind lignin processing. Almost complete liquefaction (98 %) was observed and the aromatic yield increased almost 8-fold, retaining a 96 % selectivity for arenes. This result confirmed that inorganic base was an essential additive for successful conversion of lignin to arenes.

Subsequent recycles of the $Mo_2C_{1-x}N_x$@TiN catalyst sample using the Protobind & NaOH combination were carried out. The spent catalyst was washed with water and redried at 70 °C between cycles. Over 3 cycles the catalyst maintained its high selectivity for arenes and overall yield, as well as completely liquefying the substrate (Table S4). No apparent change in the catalyst composition or crystallinity was observed by XRD after these runs (See Fig. S1). Thus, the robustness of the catalyst and reliability of the process were demonstrated, and the importance of a base, whether derived from the inherent composition of the substrate or added, for the successful processing of lignin, was established.

3.4. Elucidating the roles of ethanol

In 2014 and 2017, Li and co-workers reported that molybdenum carbide catalysts and supercritical ethanol alone simply generated a range of aliphatic condensates and not aromatics [21,23]. More recently, a similar observation was made for a molybdenum ethoxide catalyst [39]. We therefore did not perform a similar blank reaction during the course of our experiments. Wu and co-workers however, have recently published their observations that their MoC catalysts, supported on $CaCl_2$-templated porous carbons, will convert both lignin and ethanol to aromatics in the presence of base [40]. Given the requirement for base demonstrated with various lignins shown in Fig. 7, we examined the reactivity of supercritical ethanol with comparable amounts of base. For these reactions bulk Mo_2C was used as the catalyst so that we could compare the results of the current study to those we, and others had previously published, allowing us to draw a general set of conclusions from the data. If ethanol was able to contribute to the yield of aromatics under solvothermal catalysis, then either it (1) is a substrate for the formation of aromatic rings *de novo*; or (2) is converted to a reservoir of reactive molecular intermediates which alkylate (or alkoxylate) the aromatic nuclei already formed under the reaction conditions. To determine which was the case, a reaction was run using naphthalene (**15**) as both a test substrate and standard. As naphthalene (**15**) had never been observed in the product suites of any of our previous reactions, its use allowed us to rule out possibility (2). That is, the addition of side-chains to aromatic rings does not appear to occur after arene rings are formed. Heating **15** to 330 °C in ethanol in the presence of Mo_2C and sodium hydroxide did not lead to alkylation of the intact naphthalene nucleus. Its recovery unchanged and at effectively undiminished concentration indicated that it was both unreactive and not subject to alkylation

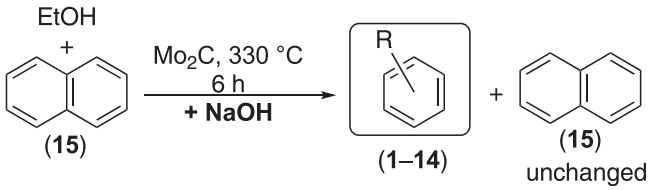

Scheme 1. Naphthalene (**15**) is inert to Mo_2C and base in supercritical EtOH, whilst the latter is apparently aromatised and deoxygenated at high temperature in the presence of Mo_2C and base.

(Scheme 1). We therefore assume other single ring arenes are similarly unreactive. Because several other alkylbenzenes were also identified at significant concentrations in the reaction mixture, it was concluded that these arenes could only have been derived from ethanol and base alone rather than from the cracking and rearrangement of naphthalene (**15**). The reactions using **15** also demonstrate that under our conditions, molybdenum carbide does not hydrogenate arenes to alicyclic compounds, as neither dialin, nor tetralin was detected.

Given that substituted arenes were formed from ethanol and base, we examined whether benzene was also a product of the process. In previous studies [18,21–23,41], benzene is not reported to be present in the product suite. Benzene is difficult to detect and quantify using standard GC & GCMS protocols due to the similarity in the boiling points of ethanol (78.4 °C) and benzene (80.1 °C). Any benzene formed in the reaction is obscured by the ethanol peak (which itself is typically removed from GC spectra in the 'solvent cut'). To determine whether benzene was indeed formed from ethanol, the product suite was analyzed from a catalytic run containing only ethanol in the presence of sodium hydroxide, over Mo_2C at 330 °C. Using the GCMS in single-ion monitoring mode, without a solvent cut unambiguously revealed the presence of the phenyl radical ion ($m/z = 77$) [42]. The presence of this signal indicated that, although not easy to observe, benzene is typically formed under reaction conditions in the presence of molybdenum carbide catalysts. Hence the arene yields reported here (and throughout the literature) are probably lower than that actually produced as non-negligible amounts of benzene are also expected to also be formed in each reaction. To determine the proportion of aromatics derived from lignin and ethanol, detailed isotopic labelling studies will be necessary in future.

The presence of benzene in the product stream is interesting, for as far as we know, this is the first time a *base-catalysed* route to all BTEX arenes from ethanol has been reported.

Studies by Szechnyi et al. are well-known for gaseous ethanol conversion to benzene, in the presence of an acidic co-catalyst or support (*e.g.* ZSM-5). These conditions facilitate dehydration of ethanol to ethene, before cyclotrimerization over Mo_2C.[43,44] Xing & Wang have also performed in-depth DFT calculations for the possible decomposition of ethanol over the (100) surface of α-Mo_2C and shown that dehydrogenation to acetaldehyde, followed by deoxygenations and cracking are all viable pathways. [45].

In our case, we hypothesize that supercritical ethanol is dehydrogenated to acetaldehyde which is able to undergo Guerbet- and Lebedev-type reactions: base-catalyzed aldol condensation with dehydration [46]. Such a scenario has been observed by *in situ* FTIR under supercritical conditions, with β-Mo_2C shown to interact with ethanol more strongly than α-MoC_{1-x} [47]. Hence our catalyst is able to effect ethanol dehydrogenation to acetaldehyde providing the initial substrate for the condensation cascade, as well source of hydrogen for subsequent hydrogenolysis steps.

Although hydrogenation to Guerbet alcohols is an expected outcome, and has been observed for supercritical ethanol in the absence and presence of Kraft lignin [22,40,47], subsequent rounds of dehydrogenation by Mo_2C and aldol addition would lead to an unsaturated, linear C_6 intermediate which could cyclize with loss of water to benzene

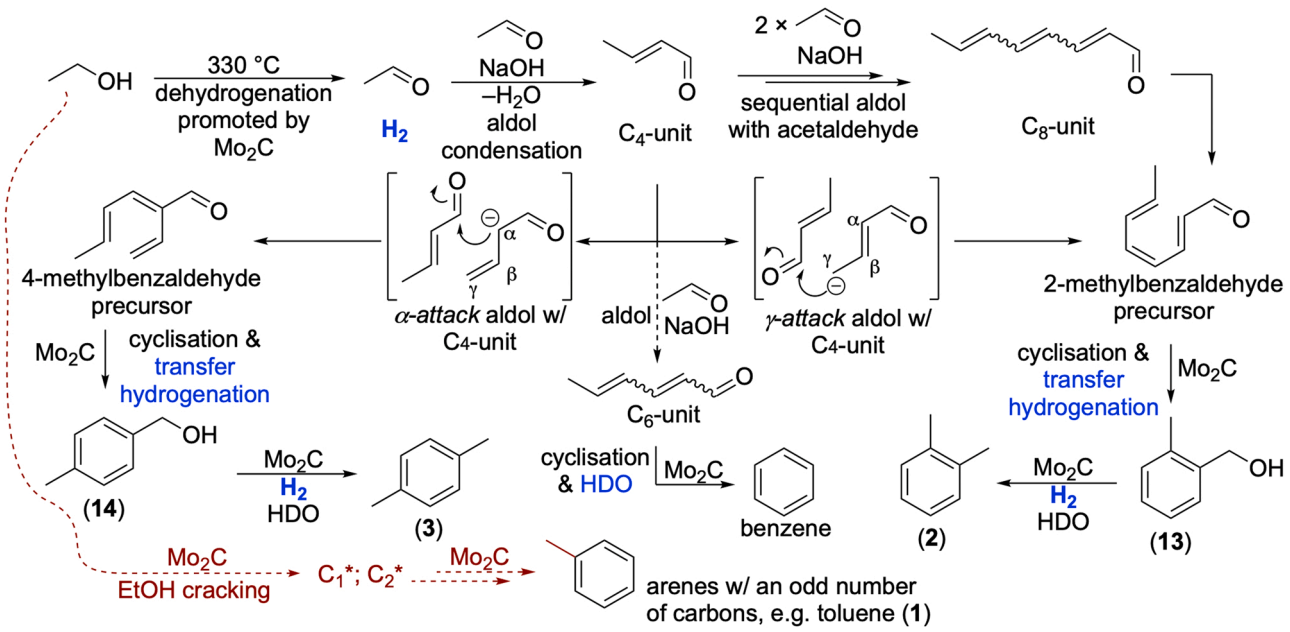

Scheme 2. Proposed pathways for the conversion of supercritical ethanol to arenes. Ethanol is both a hydrogen and carbon source in the presence of base. We speculate that concurrent processes involving cracking of ethanol lead to products containing an odd number of carbons (dashed arrows). For an in-depth discussion of ethanol conversion to 2- and 4-methylbenzaldehyde (**13** and **14**) in the presence of basic materials, see Moteki et al. [48].

(Scheme 2). Furthermore, over basic hydrotalcites gaseous ethanol (≥ 275 °C) undergoes these same aldol sequences leading to C_4 alcohols. The subsequent self-condensation of C_4 fragments results in isomers of the requisite C_8-alcohol and leads to either 2- or 4-methyl benzyl alcohol (**13** or **14**) upon cyclo-dehydrogenation (Scheme 2) [48,49]. As is evident in Table 2 (below), these isomers are present in significant quantities in the 'ethanol/base only' reactions. We propose that similar condensation, cyclization reaction sequences are not limited to gas-phase ethanol over hydrotalcite, but are much more general; occurring in the presence of base, whether it be added NaOH, or as inorganic constituents of the substrate – lignins in this study. The latter proposal is also consistent with the mechanistic studies shown in Scheme 3, below: at high temperatures, benzyl alcohols **13** and **14** deoxygenate to xylenes (**2** and **3**, respectively).

The thorough and clear mechanistic investigations of ethanol conversion over hydrotalcite by Moteki *et al.* also allow us to rule out [4 + 2] cycloadditions of unsaturated C_4 and C_2 alcohols as a pathway

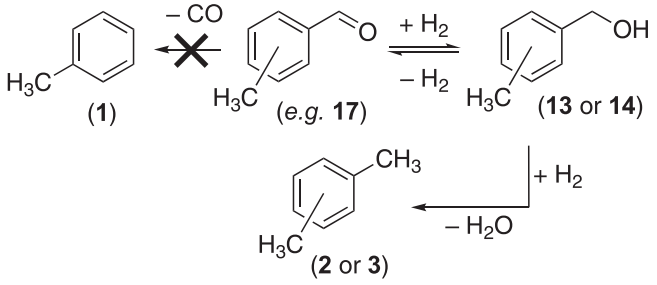

Scheme 3. Proposed defunctionalisation pathway (catalysed or uncatalyzed) for benzaldehydes and benzyl alcohols in supercritical ethanol.

Table 2
Alkyl arenes quantified (**in mg**) from mechanistic studies using various substrate probes at 330 °C over Mo_2C with ethanol as solvent/reactant.[a]

Aromatic Product	Napthalene (15)/NaOH 55 mL scale	55 mL EtOH/ NaOH	β-O-4 cross-link (16)/NaOH 55 mL scale	100 mL EtOH/ NaOH	Kraft lignin (not dried) 100 mL scale
Toluene (**1**)	18	47	171	52	133
o-Xylene (**2**)	35	107	112	122	135
p-Xylene (**3**)	19	53	60	65	70
Ethylbenzene (**4**)	10	trace	27	26	23
Propylbenzene (**5**)	3	4	15	4	18
3-Ethyltoluene (**6**)	11	4	69	14	58
C_9 isomer (**7**)	3	0	6	0	16
Other C_9 isomers	–	17[b]	–	18[b]	–
1-Ethyl-2,4-dimethylbenzene (**8**)	4	5	9	10	34
C_{10} isomer (**9**)	10	33	27	38	0
C_{10} isomer (**10**)	2	6	5	18	12
C_{10} isomer (**11**)	0	0	7	0	0
Benzyl alcohol (**12**)	22	67	54	62	28
2-Methylbenzyl alcohol (**13**)	23	130	19	110	14
4-Methylbenzyl alcohol (**14**)	17	63	29	55	0
Total	**177**	**536**	**610**	**594**	**541**

[a] Conditions as per Table 1 at 330 °C for all reactions; quantified by GC-MS as per the Experimental Procedure
[b] Total mg for all observed C_9 isomers, that were neither (**6**) nor (**7**)

for the formation of 6-membered ring skeletons directly. In comparison to the aldol–cycloaromatization pathway, the rates of Diels–Alder reactions are too low [48].

The known cracking of ethanol [43,45] and potentially other intermediate compounds into reactive surface-bound species, containing odd-numbers of carbons and their incorporation into the precursors of aromatised products would account for toluene and other aromatics (C_7, C_9, etc). Both C_2 and C_1 fragments may be able to be incorporated into the one molecule as is the case in 3-ethyl toluene (**6**). However, based on the experiment with naphthalene (**15**), it would appear that concatenation of these fragments takes place before a final cyclisation and not after: the aromatic nucleus being inert to subsequent alkylation.

The result with naphthalene (**15**) depicted in Scheme 1, prompted us to explore the synergy between substrate conversion and ethanol aromatization further. Experiments with only ethanol as the carbon source, in the presence of base, were performed and compared with the results already obtained. The yield and identity of the aromatics produced are shown in Fig. 8 & Table 2. For the reaction depicted in Scheme 1, the yield of alkylarenes was rather low in the presence of naphthalene (**15**). A total of 177 mg was quantified, being far less than observed when only ethanol was present (536 mg). Such a large difference indicated that not only was naphthalene (**15**) inert to alkylation, but that its interaction with the Mo_2C was competitively inhibiting the interaction of ethanol with the catalyst. A simple geometric calculation based on the molecular surface of naphthalene (See Supporting Information) and the assumption that it lies flat on the catalyst indicated that the 550 mg used in the reaction had a combined surface area hundreds of times larger than the measured BET surface area of the Mo_2C.

An improvement in total aromatic yield was observed when a β-O-4 cross-link (1-(3,4-dimethoxyphenyl)−2-(2-methoxyphenoxy)propane-1,3-diol, **16**) was reacted as a simple model substrate (further mechanistic investigation with this substrate are detailed in Scheme 6). Complete liquefaction occurred in a reaction on the same scale as the naphthalene and 'ethanol/base only' reactions (550 mg of substrate & 140 mg NaOH in 55 mL ethanol). The results are shown in Scheme 6, *right arrow*, and Fig. 8 & Table 2, *column 4*. Taken together with the other results in this series, this is a clear indication that both the substrate and ethanol are capable of synergistic conversion to aromatics over molybdenum carbide catalysts under basic conditions.

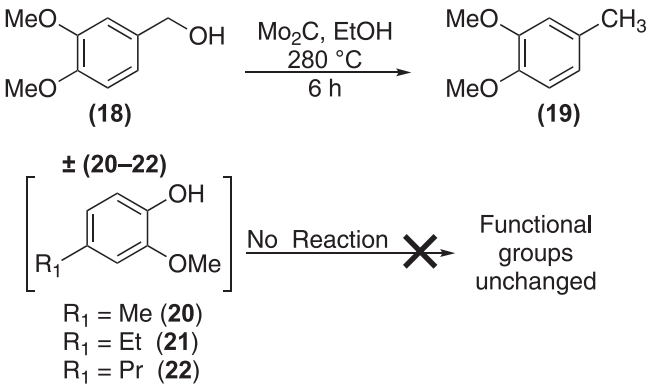

Scheme 4. Conversion of 3,4-dimethoxybenzyl alcohol (**18**) in the presence or absence of other oxygenate functionalities in supercritical ethanol over Mo_2C at 280 °C.

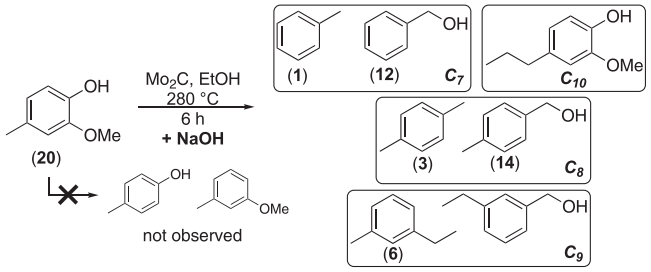

Scheme 5. Conversion of 4-methyl guaiacol (**20**) to a range of C_7–C_{10} products in basic supercritical ethanol (numbered products also observed in the hydrogenolysis of Kraft lignin as per Fig. 6).

The 610 mg of mostly deoxygenated arenes observed from the conversion of lignin model **16** is greater in mass that the 550 mg of starting material and hence some of the products must come from ethanol. The extent of the synergy however, was not straightforward to quantify. For example, assuming complete hydrodeoxygenation of the 550 mg of

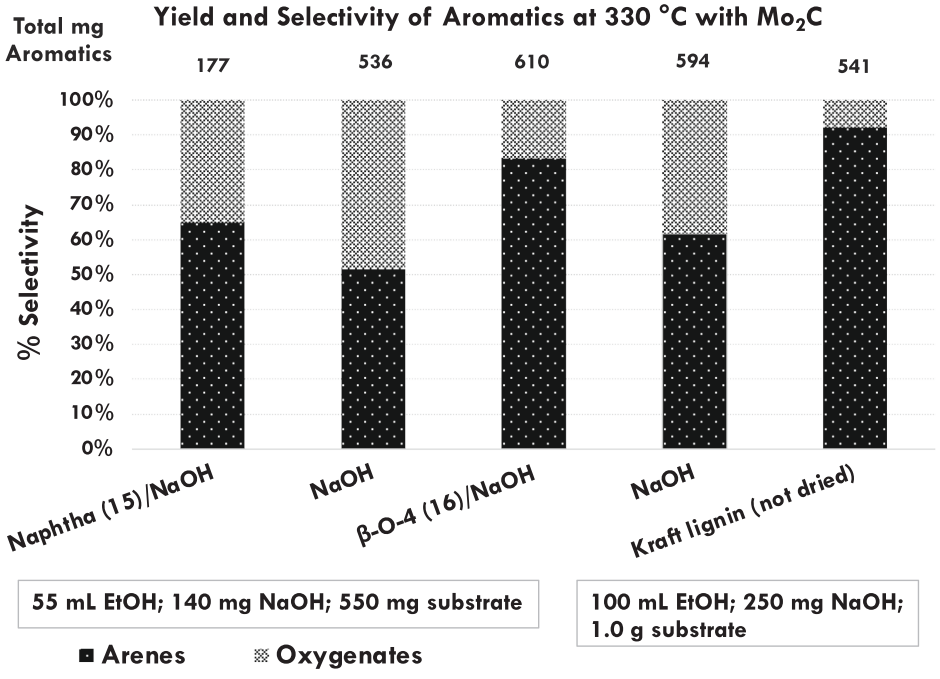

Fig. 8. Yields and selectivities of aromatics derived from ethanol and base with or without substrates using Mo_2C in supercritical ethanol at 330 °C.

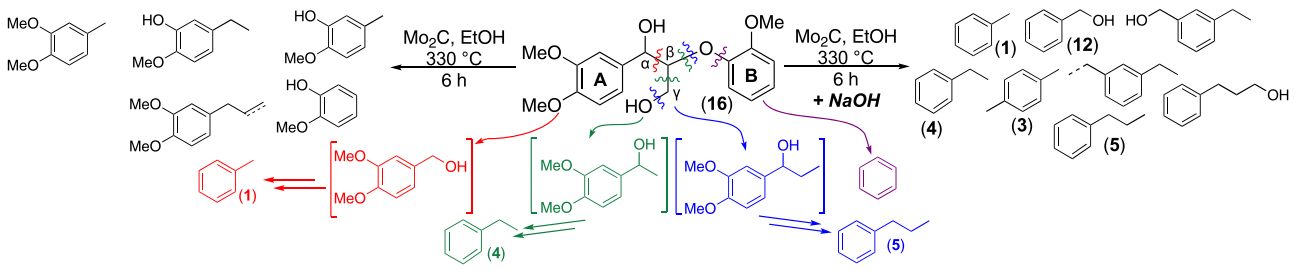

Scheme 6. Catalytic conversion of β-O-4 linkage model (**16**) in the absence & presence of added base (numbered products also observed in the hydrogenolysis of Kraft lignin as per Fig. 6).

substrate **16**, one could expect conversion of the "A-ring" to 198 mg of propyl benzene (**5**), or 175 mg of ethylbenzene (**4**), or 152 mg of toluene (**1**). Addition of any of these masses (or combinations thereof) to what is expected from ethanol (536 mg) would give a total aromatics yield of approximately 700 mg. Further difficulty in quantifying the total arene content arose when looking at the "B-ring" of **16** (Scheme 6, below). Complete hydrodeoxygenation of this portion of the molecule leads to benzene. The limitations in detecting benzene using our GCMS protocol prevented an accurate measurement of this product as discussed above. Measurement uncertainties aside, it seems clear by comparing Table 2 *columns 3 & 4*, that conversion of model compound **16** to single ring aromatics is not strictly additive with ethanol conversion under equivalent conditions.

Scaling up the 'ethanol/base only' reaction to one which is directly comparable with the reactions involving 1 g of lignin was then undertaken by increasing the amount of catalyst and base accordingly. Although the scale for the run in Fig. 8 & Table 2, *column 5* is 182 % larger than that in *column 3*, the yield of aromatics scaled by only 111 %. Given the catalysts had been shown to be recyclable, with little loss of activity in the presence of lignin, it is unlikely that this observed diminution in product yield is due to irreversible catalyst poisoning. Possibly under batch conditions, an equilibrium is reached in which the aromatics compete with ethanol for the catalyst surface and the rates of aromatization and lignin depolymerization are diminished progressively. However, the origin of this decrease in activity with scale is yet to be determined.

Interestingly, when 1 g of Kraft lignin was reacted under these conditions, the total yield of aromatics demonstrably decreased compared to the comparable 'ethanol/base only' run. (Fig. 8 & Table 2, *column 6 vs column 5;* also reported in Table 1). The liquefaction of the Kraft lignin in this run was only 82 %, indicating that a significant proportion of potentially insoluble material was present that could have competitively blocked the surface of the catalyst in an analogous fashion to naphthalene (**15**). These results therefore confirmed the advantage of using our $Mo_2C_{1-x}N_x$@TiN catalyst which displays high depolymerization capability for basic lignins, *i.e.*, 100 % liquefaction at 330 °C.

Looking further at the results in Table 2, it is apparent that despite the *ca.* 10 % difference in total aromatic yield between the 'ethanol/base only' reactions (*column 3 vs column 5*), the proportion of arenes and oxygenates in both cases was similar and selectivity for oxygenates was increased compared with experiments when lignin or model compound **16** were present. In particular, 2-methylbenzyl alcohol (**13**) stood out as one of the main oxygenated aromatics formed directly from ethanol and its prominence was also consistent with the relatively high levels of its deoxygenation product, *o*-xylene (**2**), present in every reaction. A similar arene:oxygenate selectivity was also observed in the presence of naphthalene (**15**) to the 'the ethanol/base only' reactions, providing further support for the observation that **15** was not a productive substrate for molybdenum carbide catalysis.

In contrast, the selectivity to arenes increased markedly in the presence of a productive substrate, such as lignin or the β-O-4 model compound (**16**). The bulk of this selectivity change was due to the large relative increases in toluene (**1**) observed in the presence of these substrates. A more moderate increase in ethyltoluene (**4**) and similar diminishment in 4-methylbenzyl alcohol (**14**) also contributed to the shift in selectivity towards arenes.

With the role of base firmly established as being critical for both ethanol aromatization, and high levels of lignin liquefaction, we turned our attention to mechanistic studies with simple model compounds, bearing representative functional groups.

3.5. Reaction cascades & mechanistic studies

In 2019, Li and co-authors reported on the activity of β-Mo_2C on a graphite support for the conversion of Kraft lignin to aromatics [50]. The authors concluded from their studies that alkyl arenes arise from a reaction sequence in which aryl aldehydes are hydrogenated to benzyl alcohols, which are subsequently hydrogenolysed. As discussed above, this deoxygenation was more extensive at 330 °C compared with reactions run at 280 °C. This result is in agreement with the results of our lignin studies (Table 1) and investigations using model compound below. In our hands however, the addition of a catalyst was unnecessary to effect hydrodeoxygenation of the benzyl alcohol functionality. 4-Methylbenzyl alcohol (**14**) was used as a typical substrate and was completely converted to *p*-xylene (**3**), after only 1 h at 330 °C in supercritical ethanol in the absence of added catalyst or support. Although catalytic effects of the reactor wall cannot be definitively ruled out in this thermal solvolysis [51], as Hastelloy C contains *ca.* 16 % molybdenum, it is probable that the benzyl alcohols observed in the product stream from the lignin processing reactions are intermediates that would eventually become converted to alkyl benzenes if the reaction were run for a longer time (or at higher temperatures).

Molybdenum catalysts are well-established for dehydrogenation. For example, Oyama and co-workers demonstrated that the support interactions with molybdenum(VI) oxide were crucial for improving catalytic performance for cracking and dehydrogenating ethanol [52]. Similarly, molybdenum hemicarbide is known to facilitate this process [43]. Given that there is ample precedence for spontaneous ethanol dehydrogenation to acetaldehyde under supercritical conditions [21,22] it is also possible that benzyl alcohols are similarly dehydrogenated to benzaldehydes as well as undergoing hydrogenolysis [53].

To that end, *o*-tolualdehyde (**17**) was subjected to Mo_2C catalysis in supercritical ethanol under the same conditions used to process lignin and found to selectively furnish *o*-xylene (**2**). This test not only determined that lignin fragments bearing benzaldehyde functionality could participate in the conversion to alkyl arenes, but also that they were not likely to be decarbonylated under the reaction conditions. Toluene (**1**) was not observed in the product stream of this reaction (Scheme 3).

Based on the above investigation, we concluded that the observed methyl benzenes in the product suite from our lignin hydrogenolyses at 330 °C were obtained from benzyl alcohol precursors. Incomplete deoxygenation at 280 °C, was therefore responsible for the greater proportion of benzyl alcohols observed in the oxygenate fraction of the aromatic product stream.

Kraft and other lignins contain significant numbers of methoxy- and phenolic groups [54]. Hence it was of interest to determine how these groups behaved under our conditions. The results of our investigations are shown Scheme 4. The deoxygenation of 3,4-dimethoxybenzyl alcohol (**18**) over Mo_2C at 280 °C in ethanol led only to 3,4-dimethoxy toluene (**19**): the methoxy groups remained intact. To more closely approximate the reaction conditions under which lignin is processed, the reaction was repeated in the presence of a mixture of phenolic compounds. 4-methyl- (**20**), 4-ethyl- (**1**), and 4-propyl-guaiacol (**1**) are all prominent products found in the hydrothermal conversion of lignin [55]. Here they were used to simulate the types of functional groups and intermediates that would be present during the course of lignin conversion. The presence of these phenolics did not change the outcome. Conversion of 3,4-dimethoxybenzyl alcohol (**18**) to 3,4-dimethoxy toluene (**19**) proceeded smoothly, however neither the free phenols nor methoxy-groups were hydrogenolysed to furnish deoxygenated arenes under these conditions (Scheme 4). The latter result indicated that a different set of reaction pathways was operating in this case, than does when basic Kraft and other lignins were employed as substrates.

Given that the substrate mixture above was less diverse and less impure than Kraft lignin, which itself was successfully deoxygenated by our catalysts, a lack of functional group tolerance was not the most likely explanation for the poor performance of Mo_2C under the conditions shown in Scheme 4. The main difference between the above reaction conditions and those leading to selective arene formation corresponding to Fig. 6, was, again, whether an inorganic base was present.

Using 4-methylguaiacol (**20**) as a model substrate, further investigation into the influence base had on substrate defunctionalization was undertaken. In the presence of sodium hydroxide and under otherwise identical conditions to those depicted in Scheme 4, reductive cleavage of the methoxy-groups and phenol hydroxyl-group was observed. As previously observed at 280 °C, partial deoxygenation occurred leading to a mixture of arenes and oxygenates. The product suite was significantly more varied than expected. Rather than just the starting material (**20**), toluene (**1**) and partially deoxygenated intermediates (*i.e. p*-cresol and 3-methoxytoluene) being present, the majority of the products had carbon skeletons that appeared to be the result of rearrangement or were augmented by 1–3 carbons (Scheme 5). The fact that only 2 of the 7 products possessed the expected C_7 skeletons and the others were C_8–C_{10} was further evidence that these additional carbons were derived from the ethanol solvent rather than from the methyl-groups cleaved from the substrate.

In order to investigate the efficacy of base for deoxygenation at 330 °C on a pure, lignin-like compound, **16**, a β-O-4 lignin model was synthesized according to published procedures [29] (See Supporting Information) and employed as a test substrate under both neutral and basic conditions.[2] A qualitative picture of the reaction outcome was obtained through GCMS analysis. Under neutral conditions, complete conversion of the model compound (**16**) was observed, and the product suite contained the fragments arising from the cleavage of the β-O-4 cross-link (Scheme 6, *left arrow*). In line with the results shown in Scheme 4, the dimethoxy- and guaiacol functionalities remained intact, whereas any benzylic alcohol intermediates were deoxygenated to alkyl substituents.

Conversely, in the presence of added base, the substrate (**16**) was converted to a diverse set of aromatics, the majority of which were deoxygenated (Scheme 6, *right arrow*). Whilst two benzylic alcohols (and even 3-phenylpropanol) were observed, the methoxy groups were completely hydrogenolysed. See Table S5 in the Supporting Information for further details, and above in Fig. 8 & Table 2**,** *column 4*.

The various substituents within the product suite indicated that multiple fragmentation pathways existed. Looking at the "A-ring" (Scheme 6) of substrate (**16**), cleavage between the α- and β-carbons gives rise to a benzylic alcohol intermediate and hence toluene (**1**) following complete hydrodeoxygenation (Scheme 6: *red, bottom-left pathway*). As previously discussed, toluene (**1**) is also an expected product from the aromatization of ethanol under basic conditions and hence the 171 mg total toluene (**1**) observed is expected to have originated from both the solvent and the substrate.

Base-assisted cleavage between the β- and γ-carbons of (**16**), in combination with C_β–O bond cleavage, leads directly to an aromatic ring with an ethyl substituent (*e.g.* **4**, Scheme 6: *green, bottom-mid-left pathway*). If C_β–O bond cleavage and alcohol hydrogenolyses occur, the propyl substituted arenes (*e.g.* **5**) would result (Scheme 6: *blue, bottom-mid-right pathway*). Observed unsaturation in the 3-carbon side-chain of related products is rationalized by dehydration and alkene migration events at high temperature. Hydrodeoxygenation of the "B-ring" would ultimately give benzene which is not expected to be observed routinely (Scheme 6: *purple, bottom-right pathway*).

These results are complimentary to the vapour-phase study by Lee et al. which established that anisole can be successfully converted to benzene over a Mo_2C catalyst in the presence of H_2 below 250 °C, due to its high selectivity for C–O bond cleavage (Scheme 7). Selective cleavage of the aromatic carbon–oxygen bond to furnish the arene rather than cleavage of the methyl–oxygen bond (which would give phenol) occurs despite the increased strength of the former (*ca.* 422 *vs. ca* . 339 kJ per mole). [56].

Our results here confirmed that the presence of base was essential for the deoxygenation of stable functionalities such as methoxy groups, ubiquitous in lignin. Moreover, base appears to promote deoxygenation at lower temperatures than would otherwise be the case. For example in their lignin processing work, Chen et al. observed complete selectivity to arenes using silicon carbide catalysts [37]. However, these reactions had to be conducted at 500 °C and hence the observation of very low levels of oxygen in their aromatic products was consistent with the general trend we observed for molybdenum carbide catalysts when the reaction temperature was increased from 280 °C to 330 °C.

Furthermore, the best arene yield reported by Chen et al. was *ca.* 44 mol % of the liquefied products and many of the identified products were benzene rings bearing ethyl (and ethenyl) groups. Given the high temperature involved and reactive nature of ethanol, it was unclear what proportion of product mass they reported was derived directly from the solvent and what was actually from lignin. Similarly looking at our results depicted in Scheme 5 & 6, we are not yet able to quantify confidently what proportion of the arene rings we detected originated from substrate (**16**) and how much arose from the aromatization of supercritical ethanol. Future catalysis reactions using our model compounds in inert solvents may also be necessary to uncover the separate the contributions from the substrate and the solvent to the aromatic yield.

Based on the results we have obtain thus far, we speculate that the ethoxide resulting from ethanol and base may act as a nucleophilic agent for the cleavage of C–C and C–O bonds within lignin directly, and thus substrate defunctionalization is greatly facilitated. Another way base may bring about substrate defunctionalization is through its promotion of Guerbet- and Lebedev-type condensation of ethanol with concomitant increased H_2 generation from ethanol dehydrogenation. Yongdan Li and co-workers suggested the basic groups in Kraft lignin contribute to improving the efficiency of hydrogen transfer by means of a dehydrogenation reaction [47]. Further parallels on this theme are drawn from

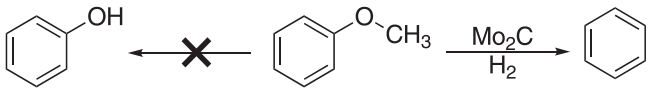

Scheme 7. Selectivity of Mo_2C for ArC–O bond cleavage in anisole, observed by Lee et al. [56].

[2] β-O-4 Lignin model (**16**), unsupported Mo_2C (88 mg), substrate (550 mg) in ethanol (55 mL) with or without sodium hydroxide (140 mg) were heated and stirred at 330 °C for 6 h.

the homogenous catalysis literature. For example, Jones and co-workers used manganese pincer complexes as Guerbet reaction catalysts for the conversion of ethanol to *n*-butanol. Without base present, the transfer hydrogenation was not detected to occur. Hence the role of the base may be to increase the hydrogen concentration to a level *in situ* so that the molybdenum catalyst can effect C–O bond hydrogenolysis selectively, as these conditions are not forcing enough for hydrogenation of the aromatic products [57].

4. Conclusions

Heterogeneous molybdenum carbide materials continue to be exceptional catalysts for the conversion of lignin and other biomolecules to renewable aromatics: simultaneously withstanding the sulfur and inorganic impurities within the substrate, whilst preserving arene nuclei by being selective for hydrogenolysis, rather than just hydrogenation. This class of catalysts also benefits from catalyst-particle–support interactions that further enhance their inherent capabilities. Our findings thus far indicate that titanium nitride is particularly effective. This may be due, in part, to titanium increasing the solubility of atomic nitrogen in molybdenum during *in situ* nitridation processes [58], leading to more intimately combined mixed phases of TiN and molybdenum carbonitride that would otherwise have been achieved on purely carbon, alumina or hydrotalcite supports.

Whilst previous reports from several groups (*e.g.* Hensen and co-workers) [18–20,41,59] have made great strides in the depolymerization of lignin under supercritical conditions and, in particular, the group of Li and co-workers have an established track record of molybdenum-catalysed lignin conversion [21–26,50], our system is the first to reveal the essential roles that the basic ash content of Kraft lignin plays during the catalysis for both defunctionalisation of intermediates to arenes, and in the conversion of ethanol to aromatic rings. Our assertion here is that this source of base plays a more significant role during lignin conversion than the use of a basic oxide support for the catalyst. From the results with Organosolv and Protobind lignins (Fig. 7), it is clear that the presence of their acidic groups inhibits the proposed aldol pathways that lead to arene formation from ethanol. These lignins can still be processed efficiently under supercritical reaction conditions in the presence of sufficiently basic media, although the total amount of added base is yet to be optimized.

The combination of basic conditions in supercritical ethanol as a reactive medium, provides both carbon and hydrogen to the aromatic product suite. As a result, this multi-parameter system has the potential to be tuned for high outputs of renewable arenes. The complex interactions between reaction components has meant that until now the key insight that aromatics arise directly from the synergistic conversion of *both* the lignin substrate *and* the ethanol when base is present, has been largely, if not completely, overlooked. Our results clearly indicate that ethanol is ultimately a significant source of additional aromatics (unknowingly) incorporated in the yields reported by us and others.

This observation alone explains why aromatic yields are higher than expect for Kraft lignin and why the product suite is so similar across all the reactions studied.

Furthermore, benzene is also expected to be produced in appreciable amounts under basic catalysis and hence most of us working in this field are likely under-reporting our arene yields and selectivities. We hope that quantitation (and appropriate safety aspects) relating to benzene will be addressed by all research groups in future studies.

Based on the insights disclosed here, there appears to be considerable scope to understand lignin to arene conversion mechanisms under supercritical conditions. Lignin processing is still a challenge and hence there is a continued need for reliable methods for complete depolymerization under reducing conditions into small molecules, rather than high molecular weight oligomers that are soluble in the reaction media, but non-volatile.

The extent of the synergy between lignin and ethanol is of particular importance. This includes investigating more fully to what extent the catalyst is able to crack ethanol, resulting in the addition of odd-numbered carbon units to the reaction intermediates, which end up as toluene (**1**), propylbenzene (**5**) and other C_9-isomers (**6**–**7**), etc (See Fig. 6 for compound numbering).

As a significant amount of ethanol self-condensation products are aliphatic, continued optimization of the catalyst and reactor systems, specifically for ethanol conversion, are expected to boost the selectivity for aromatics products.

The behaviour of supercritical ethanol and the above line of mechanistic enquiry also suggests that there is the potential for other, common renewable oxygenates to be similarly suitable for conversion to deoxygenated aromatics and related platform chemicals neat or in the presence of ethanol.

CRediT authorship contribution statement

Matthew Lui: Methodology, Investigation, Validation, Writing - Original Draft, Writing-Reviewing and Editing, Visualisation, Funding, **Anthony Masters**: Resources, Writing- Reviewing and Editing, Supervision, Funding, **Thomas Maschmeyer**: Resources, Writing- Reviewing and Editing, Supervision, Funding, **Alexander Yuen**: Conceptualisation, Investigation, Writing - Original Draft, Writing- Reviewing and Editing, Visualisation, Supervision, Project Administration.

Declaration of Competing Interest

The authors declare that they have no known competing financial interests or personal relationships that could have appeared to influence the work reported in this paper.

Data availability

Data will be made available on request.

Acknowledgements

The authors acknowledge the facilities, and the scientific and technical assistance of Hongwei Liu at Sydney Microscopy & Microanalysis, the University of Sydney node of Microscopy Australia.

The authors also acknowledge the facilities and the technical and scientific assistance of Sydney Analytical, a core research facility at The University of Sydney. Dr Jyah Strachan is acknowledged for his assistance with PXRD analyses, and Dr. Edwin Clatworthy for discussions and initial electron microscopy analyses. Financial support from Hong Kong Baptist University (Tier 1 Grant) for MYL is also acknowledged.

Appendix A. Supporting information

Supplementary data associated with this article can be found in the online version at doi:10.1016/j.apcatb.2022.122351.

References

[1] A.F. Sousa, C. Vilela, A.C. Fonseca, M. Matos, C.S.R. Freire, G.-J.M. Gruter, J.F. J. Coelho, A.J.D. Silvestre, Polym. Chem. 6 (2015) 5961–5983.
[2] B. Saake, R. Lehnen, Lignin, in: Ullmann's Encyclopedia of Industrial Chemistry, Wiley-VCH Verlag GmbH & Co. KGaA, Weinheim, 2012.
[3] R. Rinaldi, R. Jastrzebski, M.T. Clough, J. Ralph, M. Kennema, P.C.A. Bruijnincx, B. M. Weckhuysen, Angew. Chem. Int. Ed. 55 (2016) 8164–8215.
[4] N. Mahmood, Z. Yuan, J. Schmidt, C. Xu, Bioresour. Technol. 139 (2013) 13–20.
[5] J. Zakzeski, P.C.A. Bruijnincx, A.L. Jongerius, B.M. Weckhuysen, Chem. Rev. 110 (2010) 3552–3599.
[6] K.H. Kim, R.C. Brown, M. Kieffer, X. Bai, Energy Fuels 28 (2014) 6429–6437.
[7] M. Otromke, R.J. White, J. Sauer, Carbon Resour. Convers. 2 (2019) 59–71.
[8] W. Jiang, G. Lyu, Y. Liu, C. Wang, J. Chen, L.A. Lucia, Ind. Eng. Chem. Res. 53 (2014) 10328–10334.
[9] P. Ghorbannezhad, M.D. Firouzabadi, A. Ghasemian, P.J. de Wild, H.J. Heeres, J. Anal. Appl. Pyrolysis 131 (2018) 1–8.

[10] Q. Meng, J. Yan, R. Wu, H. Liu, Y. Sun, N. Wu, J. Xiang, L. Zheng, J. Zhang, B. Han, Nat. Commun. 12 (2021) 4534.
[11] R.J. Sheehan, Terephthalic acid, dimethyl terephthalate, and isophthalic acid. Ullmann's Encyclopedia of Industrial Chemistry, Wiley-VCH Verlag GmbH & Co. KGaA, Wenheim,, 2011.
[12] P.M. Lorz, F.K. Towae, W. Enke, R. Jäckh, N. Bhargava, W. Hillesheim, Phthalic acid and derivatives, in: Ullmann's Encyclopedia of Industrial Chemistry, Wiley-VCH Verlag GmbH & Co. KGaA, Wenheim, 2007.
[13] K.A. Goulas, M. Shiramizu, J.R. Lattner, B. Saha, D.G. Vlachos, Appl. Catal. A: Gen. 552 (2018) 98–104.
[14] K.U. Ingold, Aldrichimica Acta 22 (1989) 69–74.
[15] J. Maul, B.G. Frushour, J.R. Kontoff, H. Eichenauer, K.-H. Ott, C. Schade, Polystyrene and styrene copolymers, in: Ullmann's Encyclopedia of Industrial Chemistry, Wiley-VCH Verlag GmbH & Co. KGaA, Wenheim, 2007.
[16] E.H. Lee, Catal. Rev. 8 (1974) 285–305.
[17] S.I. Pérez-Uresti, J.M. Adrián-Mendiola, M.M. El-Halwagi, A. Jiménez-Gutiérrez, Processes 5 (2017) 33–42.
[18] X. Huang, T.I. Korányi, M.D. Boot, E.J.M. Hensen, ChemSusChem 7 (2014) 2276–2288.
[19] X. Huang, C. Atay, J. Zhu, S.W.L. Palstra, T.I. Korányi, M.D. Boot, E.J.M. Hensen, ACS Sustain. Chem. Eng. 5 (2017) 10864–10874.
[20] X. Huang, T.I. Korányi, M.D. Boot, E.J.M. Hensen, Green. Chem. 17 (2015) 4941–4950.
[21] R. Ma, W. Hao, X. Ma, Y. Tian, Y. Li, Angew. Chem. Int. Ed. 53 (2014) 7310–7315.
[22] X. Ma, R. Ma, W. Hao, M. Chen, F. Yan, K. Cui, Y. Tian, Y. Li, ACS Catal. 5 (2015) 4803–4813.
[23] F. Yan, R. Ma, X. Ma, K. Cui, K. Wu, M. Chen, Y. Li, Appl. Catal. B: Environ. 202 (2017) 305–313.
[24] F. Mai, Z. Wen, Y. Bai, Z. Ma, K. Cui, K. Wu, F. Yan, H. Chen, Y. Li, Ind. Eng. Chem. Res. 58 (2019) 10255–10263.
[25] Y. Bai, K. Cui, Y. Sang, K. Wu, F. Yan, F. Mai, Z. Ma, Z. Wen, H. Chen, M. Chen, Y. Li, Energy Fuels 33 (2019) 8657–8665.
[26] Y. Sang, M. Chen, F. Yan, K. Wu, Y. Bai, Q. Liu, H. Chen, Y. Li, Ind. Eng. Chem. Res. 59 (2020) 7466–7474.
[27] L. Cattelan, A.K.L. Yuen, M.Y. Lui, A.F. Masters, M. Selva, A. Perosa, T. Maschmeyer, ChemCatChem 9 (2017) 2717–2726.
[28] T. Aro, P. Fatehi, ChemSusChem 10 (2017) 1861–1877.
[29] D.W. Cho, R. Parthasarathi, A.S. Pimentel, G.D. Maestas, H.J. Park, U.C. Yoon, D. Dunaway-Mariano, S. Gnanakaran, P. Langan, P.S. Mariano, J. Org. Chem. 75 (2010) 6549–6562.
[30] M. Pang, X. Wang, W. Xia, M. Muhler, C. Liang, Ind. Eng. Chem. Res. 52 (2013) 4564–4571.
[31] Y. Zhao, K. Kamiya, K. Hashimoto, S. Nakanishi, Angew. Chem. Int. Ed. 52 (2013) 13638–13641.
[32] N.S. Kopachevska, A.K. Melnyk, I.V. Bacherikova, V.A. Zazhigalov, K. Wieczorek-Ciurowa, Khimiya, Fiz. ta Tekhnolohiya Poverkhni 6 (2015) 474–480.
[33] Fo Farges, R. Siewert, G.E. Brown Jr., A. Guesdon, G. Morin, Can. Mineral. 44 (2006) 731–753.
[34] D. Ambrose, C. Tsonopoulos, E.D. Nikitin, D.W. Morton, K.N. Marsh, J. Chem. Eng. Data 60 (2015) 3444–3482.
[35] D. Fan, X. Xie, Y. Li, L. Li, J. Sun, Chem. Eng. Technol. 41 (2018) 509–516.
[36] M. Chen, W. Hao, R. Ma, X. Ma, L. Yang, F. Yan, K. Cui, H. Chen, Y. Li, Catal. Today 298 (2017) 9–15.
[37] Y. Chen, F. Wang, Y. Jia, N. Yang, X. Zhang, Bioresour. Technol. 226 (2017) 145–149.
[38] S. Jeong, S. Yang, D.H. Kim, Mol. Catal. 442 (2017) 140–146.
[39] Q. Liu, Y. Sang, Y. Bai, K. Wu, Z. Ma, M. Chen, Y. Ma, H. Chen, Y. Li, Catal. Today (2022).
[40] K. Wu, Y. Liu, C. Yang, S. Tang, C. Liu, Y. Liu, H. Lu, B. Liang, Ind. Crops Prod. 181 (2022), 114865.
[41] T.I. Korányi, X. Huang, A.E. Coumans, E.J.M. Hensen, ACS Sustain. Chem. Eng. 5 (2017) 3535–3543.
[42] Z. Wang, M. Fingas, M. Landriault, L. Sigouin, N. Xu, Anal. Chem. 67 (1995) 3491–3500.
[43] A. Széchenyi, F. Solymosi, J. Phys. Chem. C 111 (2007) 9509–9515.
[44] A. Széchényi, R. Barthos, F. Solymosi, Catal. Lett. 110 (2006) 85–89.
[45] S.-K. Xing, G.-C. Wang, J. Mol. Catal. A: Chem. 377 (2013) 180–189.
[46] A. Chieregato, J. VelasquezOchoa, C. Bandinelli, G. Fornasari, F. Cavani, M. Mella, ChemSusChem 8 (2015) 377–388.
[47] K. Wu, C. Yang, Y. Zhu, J. Wang, X. Wang, C. Liu, Y. Liu, H. Lu, B. Liang, Y. Li, Ind. Eng. Chem. Res. 58 (2019) 20270–20281.
[48] T. Moteki, A.T. Rowley, D.T. Bregante, D.W. Flaherty, ChemCatChem 9 (2017) 1921–1929.
[49] Q.-N. Wang, X.-F. Weng, B.-C. Zhou, S.-P. Lv, S. Miao, D. Zhang, Y. Han, S.L. Scott, F. Schüth, A.-H. Lu, ACS Catal. 9 (2019) 7204–7216.
[50] K. Wu, J. Wang, Y. Zhu, X. Wang, C. Yang, Y. Liu, C. Liu, H. Lu, B. Liang, Y. Li, Ind. Eng. Chem. Res. 58 (2019) 12602–12610.
[51] V. Fábos, A.K.L. Yuen, A.F. Masters, T. Maschmeyer, Chem. – Asian J. 7 (2012) 2638–2643.
[52] W. Zhang, A. Desikan, S.T. Oyama, J. Phys. Chem. 99 (1995) 14468–14476.
[53] N. Enjamuri, S. Hassan, A. Auroux, J.K. Pandey, B. Chowdhury, Appl. Catal. A: Gen. 523 (2016) 21–30.
[54] Lignin Overview.pdf (& references therein).
[55] Y. Mathieu, L. Sauvanaud, L. Humphreys, W. Rowlands, T. Maschmeyer, A. Corma, ChemCatChem 9 (2017) 1574–1578.
[56] W.-S. Lee, Z. Wang, R.J. Wu, A. Bhan, J. Catal. 319 (2014) 44–53.
[57] N.V. Kulkarni, W.W. Brennessel, W.D. Jones, ACS Catal. 8 (2018) 997–1002.
[58] R. Sanjinés, C. Wiemer, J. Almeida, F. Lévy, Thin Solid Films 290-291 (1996) 334–338.
[59] X. Huang, C. Atay, T.I. Korányi, M.D. Boot, E.J.M. Hensen, ACS Catal. 5 (2015) 7359–7370.